Exact solution of a spin-$\frac{1}{2}$ XX chain with three-site interactions in a random transverse field: Influence of randomness on the quantum phase transition

Volodymyr Derzhko,[1] Oleg Derzhko,[2,3,4] and Johannes Richter[4]

[1]*Institute of Theoretical Physics, University of Wrocław, pl. Maksa Borna 9, 50-204 Wrocław, Poland*
[2]*Institute for Condensed Matter Physics, National Academy of Sciences of Ukraine, 1 Svientsitskii Street, L'viv-11, 79011, Ukraine*
[3]*Department for Theoretical Physics, Ivan Franko National University of L'viv, 12 Drahomanov Street, L'viv-5, 79005, Ukraine*
[4]*Institut für Theoretische Physik, Universität Magdeburg, P.O. Box 4120, 39016 Magdeburg, Germany*

We present exact results for the ground-state and thermodynamic properties of the spin-1/2 XX chain with three-site interactions in a random (Lorentzian) transverse field. We discuss the influence of randomness on the quantum critical behavior known to be present in the nonrandom model. We find that at zero temperature the characteristic features of the quantum phase transition, such as kinks in the magnetization versus field curve, are smeared out by randomness. However, at low but finite temperatures signatures of the quantum critical behavior are preserved if the randomness is not too large. Even the quantum critical region may be slightly enlarged for very weak randomness. In addition to the exact results for Lorentzian randomness we present a more general discussion of an arbitrarily random transverse magnetic field based on the inspection of the moments of the density of states.

I. INTRODUCTORY REMARKS

In recent years the theory of quantum phase transitions has been in the focus of very active research.[1–3] The quantum phase transitions take place at zero temperature by changing a control parameter and emerge as a result of competing different ground-state phases. Importantly, quantum phase transitions can influence the behavior of systems over a wide range of the phase diagram at nonzero (sometimes quite large) temperatures. Exactly solvable quantum models exhibiting a quantum phase transition are notoriously rare. A well-known example of a solvable model is the spin-1/2 Ising chain in a transverse field, where a zero-temperature transition from the ordered quantum Ising phase (small transverse fields) to the disordered quantum paramagnetic phase (large transverse fields) takes place. This model is often used for illustration of basic concepts in the quantum phase transition theory.[2,4–8] In general, spin-1/2 XY chains[9] provide an excellent ground for various statistical mechanics studies since in many cases the calculations can be performed without any approximation. Moreover, there are some real-life compounds that can be viewed as realizations of one-dimensional spin-1/2 XY models.[10–13]

Quite recently, two other classes of solvable models have been found, namely a two-dimensional Kitaev model[14] and a spin-1/2 XY chain with multisite interactions[15–17] (see also Ref. 18). The model belonging to the latter class is of interest in this paper. This model has an essentially richer ground-state phase diagram as the standard one-dimensional spin-1/2 XY model. In particular, it may exhibit several gapless spin-liquid phases and quantum phase transitions between them.[16,17]

On the other hand, quantum models with random Hamiltonian parameters present another class of models for which an exact solution cannot be found easily. A solvable model with diagonal Lorentzian disorder was introduced by Lloyd.[19] Later on Lloyd's idea was used to study random spin-1/2 XX chains.[20] Also an extension to correlated off-diagonal

Lorentzian disorder and its application to spin-1/2 XX chains was considered; see Refs. 21 and 22.

Naturally, the investigation of quantum phase transitions in systems with randomness is a challenging task. The random transverse-field Ising spin chain is known as a tractable model to study effects of quenched randomness on critical behavior.[23] Within the context of random quantum systems, exactly solvable models may play an important role. Merging together the above-mentioned solvable quantum spin models with three-site interactions and Lloyd's model of disorder we present here an exact analysis of a specific random quantum spin model. In particular, the influence of randomness on the quantum phase transition inherent in the nonrandom spin model can be studied. In the presence of randomness the quantum phase transition becomes a crossover. Our solution presented below is based on the Jordan–Wigner transformation of the spin Hamiltonian to the Hamiltonian of a tight-binding chain of spinless fermions with nearest-neighbor and next-nearest-neighbor hoppings and random (Lorentzian) on-site energy. Next-nearest-neighbor hopping is a new feature emerging owing to three-site interactions which makes further calculations more involved. We introduce Green functions and find exactly the random-averaged Green functions that yield the random-averaged density of states. We use the obtained density of states to discuss some ground-state and finite-temperature properties of the spin model. Although the random-averaged density of states can be obtained only for a specific probability distribution, the moments of the density of states can be obtained for an arbitrary inhomogeneous spin chain. These quantities can illustrate some general effects on the properties of the quantum spin chain caused by inhomogeneity and yield thermodynamic quantities in the high-temperature limit. Our exact results allow us to illustrate the effect of randomness on a quantum phase transition. In particular we discuss how a quantum critical region may be modified owing to randomness.

The paper is organized as follows. In the next sections we define the spin model under consideration (Sec. II) and

calculate the random-averaged density of states that yields thermodynamic quantities (Sec. III). Then, in Sec. IV, we discuss some properties of the spin model at zero and nonzero temperatures. We illustrate the effect of the introduced disorder for the transverse magnetization, specific heat, and static transverse susceptibility, and put our discussion in a general context of a theory of quantum phase transitions with randomness. In Sec. V we discuss some global properties of the density of states for an arbitrary inhomogeneous spin-1/2 transverse XX chain with three-site interactions. Finally, in Sec. VI, we summarize our findings.

II. THE MODEL

To be specific, we consider a linear chain of N spins with spin quantum number $s = 1/2$. Each spin interacts with spins on nearest-neighboring sites and on next-nearest-neighboring sites. Moreover, all spins interact with an external magnetic field that acquires a random value on each site. The Hamiltonian of the model reads

$$H = \sum_n \left[J \left(s_n^x s_{n+1}^x + s_n^y s_{n+1}^y \right) \right.$$
$$\left. + K \left(s_n^x s_{n+1}^z s_{n+2}^x + s_n^y s_{n+1}^z s_{n+2}^y \right) \right] + \sum_n \Omega_n s_n^z, \quad (2.1)$$

where periodic boundary conditions are implied for convenience. Here J and K are the two-site isotropic XY (i.e., XX) interaction and the three-site $XZX + YZY$ interaction, respectively, and Ω_n is the transverse field on the site n. Although exact solvability is the main motivation to consider the three-site interactions, we note that Hamiltonians similar to Eq. (2.1) may be generated in optical lattices.[24]

The on-site transverse fields are assumed to be independent random variables, each with the Lorentzian probability distribution

$$p(\Omega_n) = \frac{1}{\pi} \frac{\Gamma}{(\Omega_n - \Omega_0)^2 + \Gamma^2}, \quad (2.2)$$

where Ω_0 is the mean value and Γ controls the strength of disorder. We are interested in (random-averaged) thermodynamic quantities of spin model (2.1) and (2.2).

As the first step in the calculation of thermodynamic quantities of the spin model we perform the Jordan–Wigner fermionization[9] to transform the Hamiltonian (2.1) into a bilinear Fermi form:

$$H = \sum_n \left[\frac{J}{2} (c_n^\dagger c_{n+1} + c_{n+1}^\dagger c_n) \right.$$
$$\left. - \frac{K}{4} (c_n^\dagger c_{n+2} + c_{n+2}^\dagger c_n) + \Omega_n \left(c_n^\dagger c_n - \frac{1}{2} \right) \right]$$
$$= \sum_{n=1}^N \sum_{m=1}^N c_n^\dagger A_{nm} c_m - \frac{1}{2} \sum_{n=1}^N \Omega_n. \quad (2.3)$$

As typical for the fermionic representation of the spin model, the magnetic field (here its uniform part Ω_0) plays the role of a chemical potential. From Ref. 9 we know that the bilinear
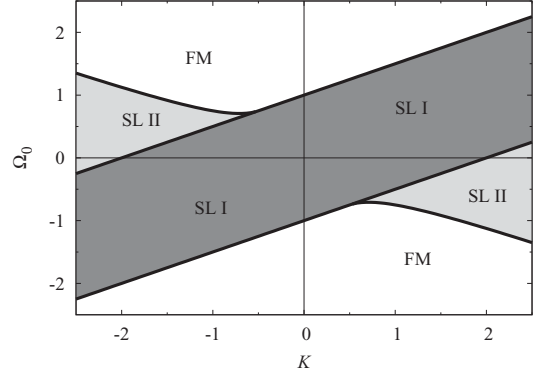

FIG. 1. The ground-state phase diagram of nonrandom model (2.1) with $J = \pm 1$ and $\Omega_n = \Omega_0$ discussed earlier in Refs. 16 and 25. Dark gray region corresponds to the spin-liquid I phase (two Fermi points), light gray regions correspond to the spin-liquid II phase (four Fermi points), and white regions correspond to the ferromagnetic phase.

form in Eq. (2.3) can be diagonalized. After performing the linear canonical transformation

$$\eta_\nu = \sum_{n=1}^N g_{\nu n} c_n, \quad \eta_\nu^\dagger = \sum_{n=1}^N g_{\nu n} c_n^\dagger,$$

$$\Lambda_\nu g_{\nu n} = \sum_{i=1}^N g_{\nu i} A_{in},$$

$$\sum_{i=1}^N g_{\nu i} g_{\mu i} = \delta_{\nu \mu}, \quad \sum_{\mu=1}^N g_{\mu i} g_{\mu j} = \delta_{ij}, \quad (2.4)$$

we find

$$H = \sum_{\nu=1}^N \Lambda_\nu \left(\eta_\nu^\dagger \eta_\nu - \frac{1}{2} \right). \quad (2.5)$$

Although this can be done in principle, finding $g_{\nu n}$ and Λ_ν is a complicated task in practice because of nonhomogeneous values of Ω_n.

Before we present the solution of the random model, for convenience we illustrate briefly the basic features of the nonrandom model, i.e., $\Omega_n = \Omega_0$ is independent of the site index n; see Refs. 16 and 25 and Fig. 1. The nonrandom model exhibits three phases. In the K–Ω_0 plane ($|J| = 1$), the spin-liquid I phase occurs in the region $-1 + K/2 < \Omega_0 < 1 + K/2$ (dark gray region in Fig. 1), the spin-liquid II phase occurs in the regions $K < -1/2$, $1 + K/2 < \Omega_0 < -K/2 - 1/(4K)$, and $K > 1/2$, $-K/2 - 1/(4K) < \Omega_0 < -1 + K/2$ (light gray regions in Fig. 1), whereas the remaining regions (white in Fig. 1) correspond to the ferromagnetic phase. The two different spin-liquid phases correspond to gapless spinless-fermion systems having two or four Fermi points, whereas the ferromagnetic phase corresponds to a gapped spinless-fermion system. Although the choice of the order parameter that in a transparent way would be associated with the modification of the Fermi surface topology is still under debate,[16,17,25,26] there is no doubt that the different phases and the transitions between them may be identified by looking at the behavior of the ground-state transverse magnetization m_z

as a function of Ω_0 or K. Several cusps in the magnetization curve indicate quantum phase transition points; see curves for $\Gamma = 0$ in Figs. 3 and 4 in Sec. IV.

III. THE AVERAGED DENSITY OF STATES AND THERMODYNAMIC QUANTITIES

The free-fermion representation of the spin model, Eq. (2.5), immediately implies simple formulas for thermodynamic quantities, as

$$f = -T \int d\omega \rho(\omega) \ln\left(2 \cosh \frac{\omega}{2T}\right),$$
$$\rho(\omega) = \frac{1}{N} \sum_{\nu=1}^{N} \delta(\omega - \Lambda_\nu), \quad (3.1)$$

for the Helmholtz free energy (per site). Here we have introduced the density of states $\rho(\omega)$. The random-averaged Helmholtz free energy $\overline{f}$ is given by Eq. (3.1) with the random-averaged density of states $\overline{\rho(\omega)}$, where $\overline{(\ldots)} = \prod_{n=1}^{N} \int d\Omega_n p(\Omega_n) (\ldots)$. Thus our task is to find $\overline{\rho(\omega)}$.

Using (3.1), (2.5), (2.4) one can easily convince oneself that

$$\rho(\omega) = \mp \frac{1}{N\pi} \sum_{j=1}^{N} \Im G_{jj}^{\mp}(\omega \pm i\epsilon), \quad (3.2)$$

where

$$G_{nm}^{\mp}(t) = \mp i\theta(\pm t)\langle\{c_n(t), c_m^\dagger\}\rangle,$$
$$G_{nm}^{\mp}(t) = \frac{1}{2\pi} \int_{-\infty}^{\infty} d\omega \exp(-i\omega t) G_{nm}^{\mp}(\omega \pm i\epsilon) \quad (3.3)$$

[$\theta(x)$ is the Heaviside step function] are the retarded and advanced temperature double-time Green functions.[27–29] On the other hand, one easily finds the following set of equations for $G_{nm}^{\mp}(\omega \pm i\epsilon)$:

$$(\omega \pm i\epsilon - \Omega_n) G_{nm}^{\mp}(\omega \pm i\epsilon)$$
$$- \frac{J}{2}[G_{n-1,m}^{\mp}(\omega \pm i\epsilon) + G_{n+1,m}^{\mp}(\omega \pm i\epsilon)]$$
$$+ \frac{K}{4}[G_{n-2,m}^{\mp}(\omega \pm i\epsilon) + G_{n+2,m}^{\mp}(\omega \pm i\epsilon)] = \delta_{nm}. \quad (3.4)$$

Because of nonhomogeneous values of Ω_n it is not possible to solve (3.4) and to find the required diagonal Green functions $G_{nn}^{\mp}(\omega \pm i\epsilon)$ that enter Eq. (3.2). However, it is well known[19] that if Ω_n is a Lorentzian random variable (2.2) the set of equations (3.4) can be averaged over random realizations, leading to a set of equation for translational-invariant random-averaged Green functions $\overline{G_{nm}^{\mp}(\omega)}$. Supposing that Ω_n is a complex variable and noticing that $G_{nm}^{-}(\omega + i\epsilon)$ [$G_{nm}^{+}(\omega - i\epsilon)$] cannot have a pole in the lower [upper] half-plane of the complex variable Ω_n, we perform the averaging with (2.2) by means of contour integrals closing the contours of integrations in the half-planes where the Green function has no poles.[19–22] As a result we obtain

$$(\omega \pm i\Gamma - \Omega_0) \overline{G_{nm}^{\mp}(\omega)} - \frac{J}{2}\left[\overline{G_{n-1,m}^{\mp}(\omega)} + \overline{G_{n+1,m}^{\mp}(\omega)}\right]$$
$$+ \frac{K}{4}\left[\overline{G_{n-2,m}^{\mp}(\omega)} + \overline{G_{n+2,m}^{\mp}(\omega)}\right] = \delta_{nm}. \quad (3.5)$$

The set of equations (3.5) possesses translational symmetry already and therefore

$$\overline{G_{nm}^{\mp}(\omega)} = \frac{1}{2\pi} \int_{-\pi}^{\pi} d\kappa \frac{\exp[i(n-m)\kappa]}{\omega - \Omega_0 - J\cos\kappa + \frac{K}{2}\cos(2\kappa) \pm i\Gamma}. \quad (3.6)$$

To evaluate the integral in (3.6) we introduce a new variable $z = \exp(i\kappa)$. Then Eq. (3.6) becomes

$$\overline{G_{nm}^{\mp}(\omega)} = \frac{1}{2\pi i}$$
$$\times \oint dz \frac{z^{n-m+1}}{\frac{K}{4}(z^4+1) - \frac{J}{2}z(z^2+1) + (\omega - \Omega_0 \pm i\Gamma)z^2}, \quad (3.7)$$

where the contour of integration runs counterclockwise along the unit circle in the complex plane z.

The calculation of (3.7) is simple if either $K = 0$ or $J = 0$, yielding $\overline{G_{nn}^{\mp}(\omega)} = 1/\sqrt{(\omega - \Omega_0 \pm i\Gamma)^2 - J^2}$ (see Ref. 20) or $\overline{G_{nn}^{\mp}(\omega)} = 1/\sqrt{(\omega - \Omega_0 \pm i\Gamma)^2 - K^2/4}$. For arbitrary values of the interaction constants, $0 < |K/J| < \infty$, we have to solve the fourth-order algebraic equation

$$z^4 - \frac{2J}{K}z^3 + \frac{4}{K}(\omega - \Omega_0 \pm i\Gamma)z^2 - \frac{2J}{K}z + 1 = 0, \quad (3.8)$$

which is a quasisymmetric one (i.e., of the form $a_0 z^4 + a_1 z^3 + a_2 z^2 + a_1 m z + a_0 m^2 = 0$ with $m = 1$). Dividing Eq. (3.8) by z^2 and using the variable change $y = z + 1/z$, we immediately find

$$y_\pm = \frac{J}{K} \pm g,$$
$$g = \sqrt{\frac{J^2}{K^2} - \frac{4}{K}(\omega - \Omega_0 \pm i\Gamma) + 2}. \quad (3.9)$$

As a result,

$$z_\pm = \frac{y \pm \sqrt{y^2 - 4}}{2}, \qquad z_+ z_- = 1, \quad (3.10)$$

where y is either y_+ or y_-. Let us denote the roots of Eq. (3.8), which are given in Eqs. (3.10) and (3.9), by z_1, z_2, z_3, z_4, $|z_1| \leqslant |z_2| \leqslant |z_3| \leqslant |z_4|$; see Appendix. Only two roots are inside the unit circle $|z| < 1$ resulting in

$$\overline{G_{nn}^{\mp}(\omega)} = \frac{4}{K}\left[\frac{z_1}{(z_1 - z_2)(z_1 - z_3)(z_1 - z_4)}\right.$$
$$\left. + \frac{z_2}{(z_2 - z_1)(z_2 - z_3)(z_2 - z_4)}\right]. \quad (3.11)$$

Then the density of states $\overline{\rho(\omega)}$ is calculated according to Eq. (3.2). The described scheme for $\Gamma = 0$ reproduces the density of states of the nonrandom model reported in Ref. 16.

Our results for $\overline{\rho(\omega)}$ for typical sets of parameters are shown in Fig. 2. We put $\Omega_0 = 0$, since a nonzero Ω_0 leads only to a trivial shift along the ω axis; see, e.g., Eq. (3.6). At the van Hove singularities present for the nonrandom model in Fig. 2 the density of states exhibits the typical one-dimensional inverse square-root singularity. For parameters Ω_0 or K, where a quantum phase transition occurs, a van Hove singularity is located at $\omega = \Omega_0$ [as in Fig. 2(b), where it is at $\omega = \Omega_0 = 0$].
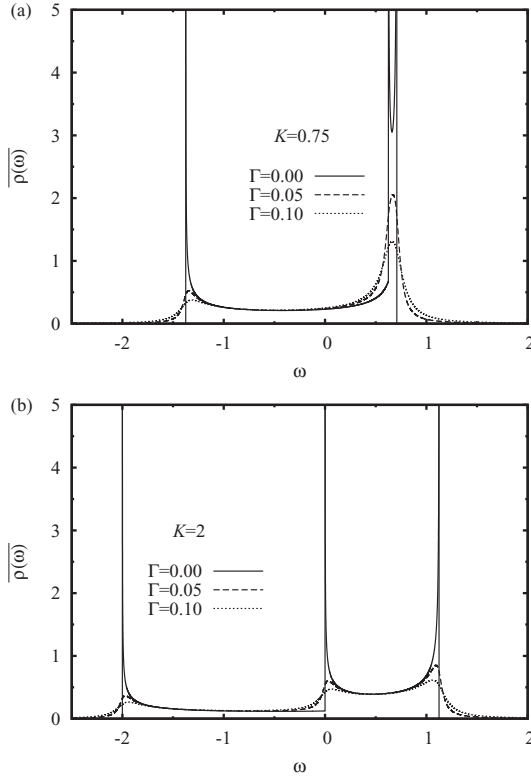
FIG. 2. The random-averaged density of states $\overline{\rho(\omega)}$ for the spin model (2.1), (2.2) with $J = 1$, (a) $K = 0.75$, (b) $K = 2$, $\Omega_0 = 0$, and (solid) $\Gamma = 0$, (dashed) $\Gamma = 0.05$, (dotted) $\Gamma = 0.1$.

The middle peak in the density of states shown in Fig. 2 (it appears if $|K| > 1/2$; see Fig. 1) indicates a quantum phase transition between the spin-liquid I and spin-liquid II phases. Small randomness leads mainly to rounding of the van Hove singularities and to the appearance of tails in the density of states above and below the band edges of the nonrandom model. With increasing Γ, the density of states becomes more and more smeared out, i.e., the fingerprints of the van Hove singularities disappear and the tails increase. These changes of the density of states due to randomness influence the ground-state and finite-temperature properties to be discussed in the next section.

Finally, it is important to note the following. A ground state of the nonrandom spin model (2.1) is generally speaking a product of one-particle (more precisely, one-fermion) states, which are plane waves. While for $\Gamma = 0$ the one-particle states within the band(s) are extended states with infinite localization length, for any small (diagonal) Lorentzian disorder, i.e., for $\Gamma > 0$, *all* one-particle states of the Hamiltonian (2.5) become localized; see e.g., Ref. 30. As a result, the nature of the quantum phases of the nonrandom model changes and the quantum phase transition inherent in the nonrandom model becomes a crossover.[31]

IV. GROUND-STATE AND THERMODYNAMIC PROPERTIES

The obtained (random-averaged) density of states permits examining various quantities characterizing behavior of the spin model at zero and nonzero temperatures; see Eq. (3.1).

For the ground-state energy, the entropy, and the specific heat we have

$$\overline{e_0} = \int d\omega \overline{\rho(\omega)} \frac{|\omega|}{2}, \tag{4.1}$$

$$\overline{s} = \int d\omega \overline{\rho(\omega)} \left[\ln \left(2 \cosh \frac{\omega}{2T} \right) - \frac{\omega}{2T} \tanh \frac{\omega}{2T} \right], \tag{4.2}$$

$$\overline{c} = \int d\omega \overline{\rho(\omega)} \left(\frac{\frac{\omega}{2T}}{\cosh \frac{\omega}{2T}} \right)^2, \tag{4.3}$$

respectively. Next, for the transverse magnetization and the static transverse susceptibility we have

$$\overline{m_z} = \frac{\partial \overline{f}}{\partial \Omega_0} = -\frac{1}{2} \int d\omega \overline{\rho(\omega)} \tanh \frac{\omega}{2T}, \tag{4.4}$$

$$\overline{\chi_{zz}} = \frac{\partial \overline{m_z}}{\partial \Omega_0} = -\frac{1}{4T} \int d\omega \overline{\rho(\omega)} \frac{1}{\cosh^2 \frac{\omega}{2T}}, \tag{4.5}$$

respectively.

In Figs. 3 and 4 we report some results for the ground-state transverse magnetization. In the ground state of the nonrandom spin system the model can be in three different phases (spin-liquid I, II, and ferromagnetic); see Refs. 16 and 25 and the discussion in Sec. II. The transitions between them can clearly be detected by the cusps in the magnetization curves in Figs. 3 and 4.

Let us briefly discuss a prominent feature of the magnetization curve, namely the steep part in the curve near saturation ($\Omega_0 \approx -0.708$) seen in Fig. 3(b) for $\Gamma = 0$. This jumplike behavior resembles the magnetization jumps observed in frustrated quantum antiferromagnets.[32] The corresponding density of states [see Fig. 2(a)] shows a narrow upper band, present for $K > 1/2$. The two singularities defining the band edges approach each other if $K \to 1/2$, i.e., the upper band becomes flat. However, by contrast to flat bands discussed in Ref. 32 the number of states in the narrow upper band of our model decreases with decreasing of bandwidth. As a result the middle cusp in the magnetization curve [see Fig. 3(b)] related to the middle singularity in the density of states [see Fig. 2(a)] moves to the left cusp this way yielding the steep part before saturation seen in Fig. 3(b). The slope of that part of the magnetization curve increases if $K \to 1/2$; however, at the same time its height decreases and vanishes finally at $K = 1/2$, where the magnetization approaches the saturation continuously with an infinite slope; see Fig. 3(a). Moreover, $1/2 - m_z \propto (\Omega_0 + 0.75)^\varepsilon$ if $\Omega_0 + 0.75 \to +0$ with $\varepsilon = 1/4$ instead of the usual value $\varepsilon = 1/2$; see Ref. 2.

The effect of randomness on the magnetization m_z is similar to that of a finite temperature. For small randomness the cusps in the $\overline{m_z}$ curves, which indicate boundaries of different ground-state phases, become rounded, indicating that a quantum phase transition present at $\Gamma = 0$ transforms into a crossover at $\Gamma > 0$. Although even small randomness is sufficient to erode the boundaries between different ground-state phases by a noticeable rounding of the cusps of $\overline{m_z}$, it may have almost no influence on $\overline{m_z}$ for parameter values corresponding to the spin-liquid phases; see Figs. 3 and 4.
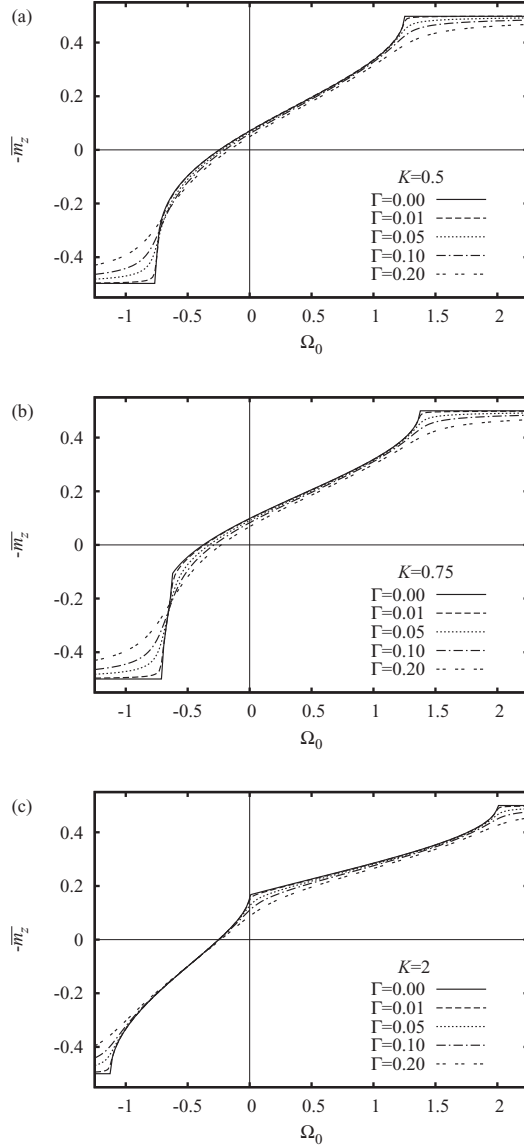
FIG. 3. Ground-state transverse magnetization $-\overline{m_z}$ (4.4) versus Ω_0 for the spin model (2.1), (2.2) with $J = 1$, (a) $K = 0.5$, (b) $K = 0.75$, (c) $K = 2$ for $\Gamma = 0, \ldots, 0.2$. The quantum phase transitions occurring in the nonrandom model (a) at $\Omega_0 = -0.75$, $\Omega_0 = 1.25$, (b) at $\Omega_0 \approx -0.708$, $\Omega_0 = -0.625$, $\Omega_0 = 1.375$, and (c) at $\Omega_0 = -1.125$, $\Omega_0 = 0$, $\Omega_0 = 2$ are signaled by kinks in the magnetization.

Other peculiarities of the nonrandom model, namely nonzero magnetization at $\Omega_0 = 0$, zero magnetization at nonzero Ω_0, as well as saturated magnetization for $|\Omega_0| < |J|$ [see Fig. 4] become less pronounced as the strength of disorder increases.

In Figs. 5 and 6 we report some of our findings for nonzero temperatures (for the sake of brevity we consider the case $\Omega_0 = 0$, only). The specific heat $\overline{c}$ for various parameter sets is presented in Fig. 5, where we show $\overline{c}/T$ as a function of temperature T. For the nonrandom case $\Gamma = 0$ it is known[16] that $c(T) \propto T$ in the limit $T \to 0$ for all K except $K = K_{\text{crit}} = \pm 2|J|$. For the critical value of K, $K = K_{\text{crit}}$, we have $c(T) \propto \sqrt{T}$.

Let us start with the discussion of the behavior of $\overline{c}/T$ for $K = 1$, i.e., the system is quite far away from the
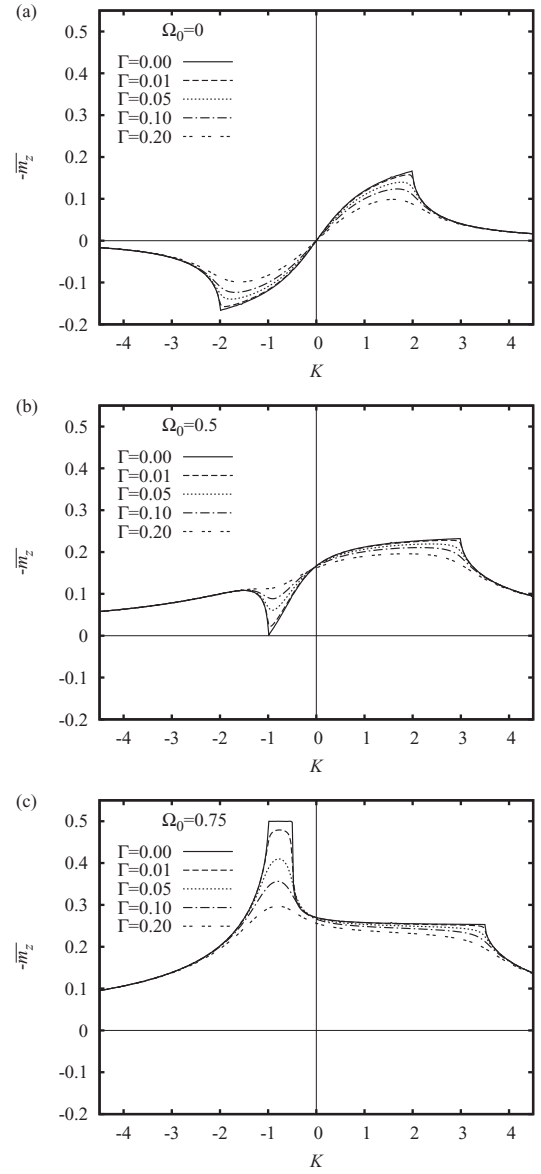

FIG. 4. Ground-state transverse magnetization $-\overline{m_z}$ (4.4) versus K for the spin model (2.1), (2.2) with $J = 1$, (a) $\Omega_0 = 0$, (b) $\Omega_0 = 0.5$, (c) $\Omega_0 = 0.75$ for $\Gamma = 0, \ldots, 0.2$. The quantum phase transitions occurring in the nonrandom model (a) at $K = -2$, $K = 2$, (b) at $K = -1$, $K = 3$, and (c) at $K = -1$, $K = -0.5$, $K = 3.5$ are signaled by kinks in the magnetization.

quantum critical point $K_{\text{crit}} = 2$. Then we have the typical high-temperature maximum in $\overline{c}(T)$ related to the relevant energy scale (depending on J and K) and a constant value of $\overline{c}/T$ at low T corresponding to $\overline{c} \propto T$. The position of the high-temperature maximum moves to higher temperatures as K increases. The overall modification of the $\overline{c}/T$ versus T curve by randomness is small. There is only a small change of the slope in the dependence $\overline{c}$ on T as $T \to 0$ and a slight shift of the height and the position of the high-temperature maximum. At the quantum critical point $K = K_{\text{crit}} = 2$ we have a completely different behavior of $\overline{c}/T$. The high-temperature maximum is still present (and again there is only a weak effect of randomness on that maximum). However, below the maximum there is an increase of $\overline{c}/T$ with decreasing
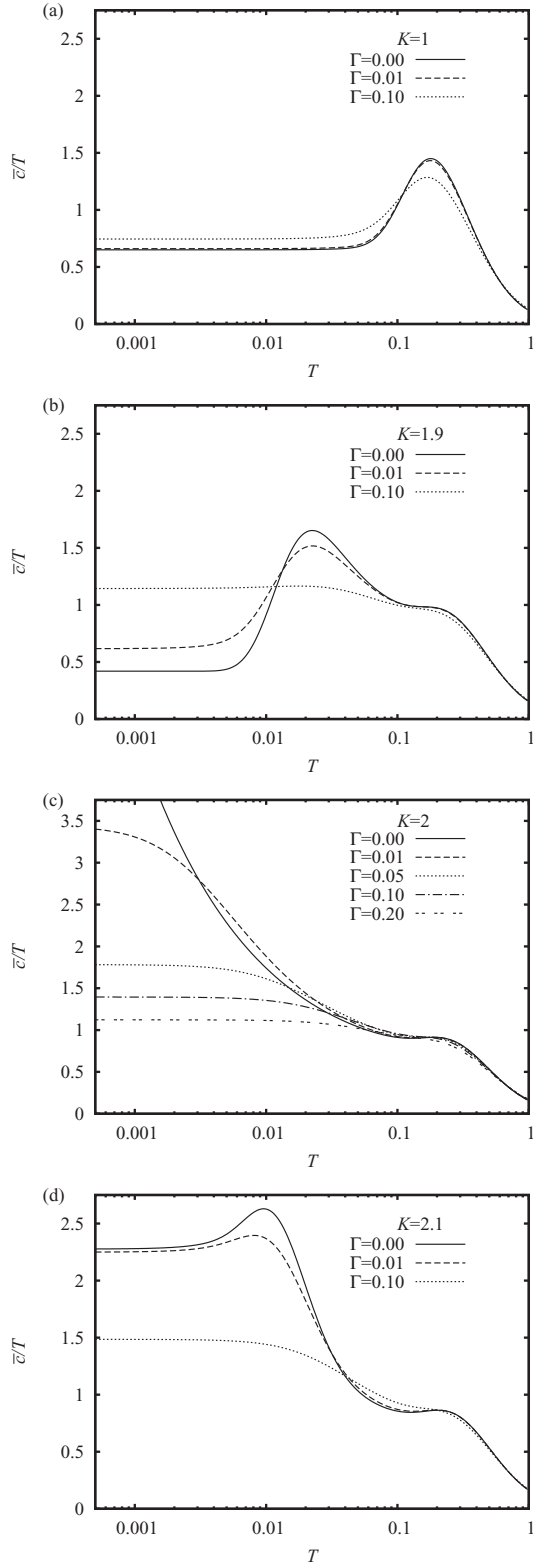
FIG. 5. $\overline{c}/T$ versus T, $\overline{c}$ is the specific heat given in Eq. (4.3), for the spin model (2.1), (2.2) with $J = 1$, $K = 1$, 1.9, 2, 2.1 (from top to bottom), $\Omega_0 = 0$, and $\Gamma = 0, \ldots, 0.2$.
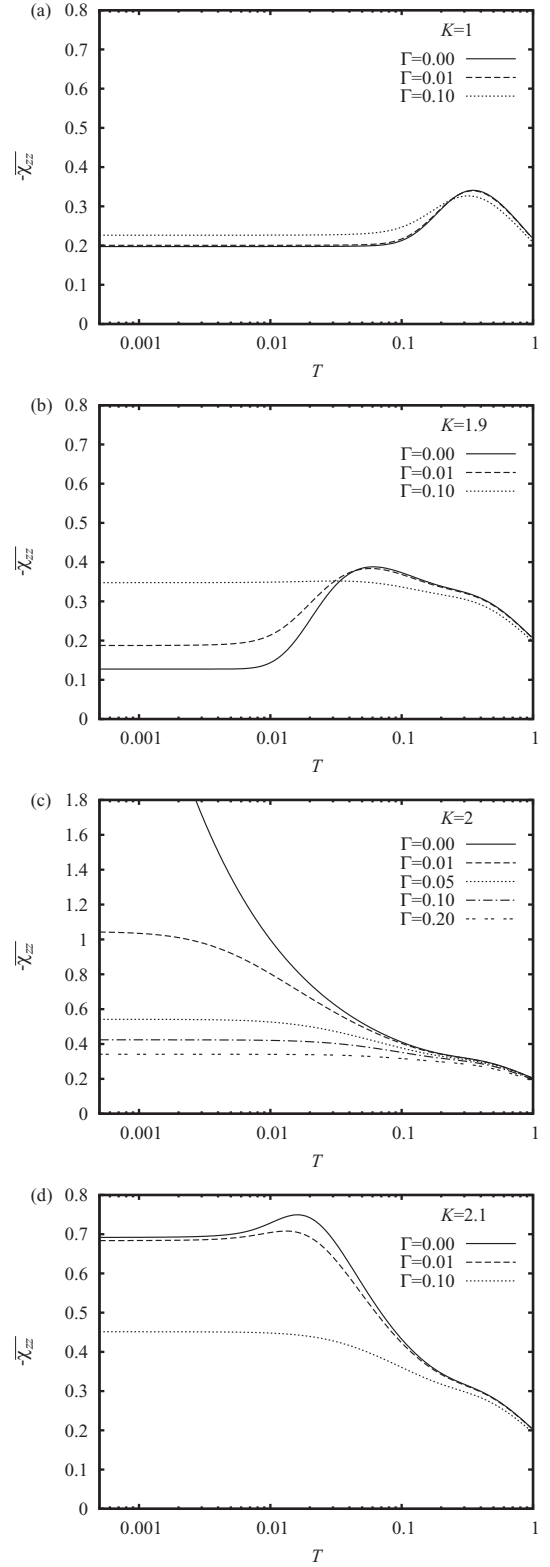
FIG. 6. Static transverse susceptibility $-\overline{\chi_{zz}}$ (4.5) versus T for the spin model (2.1), (2.2) with $J = 1$, $K = 1$, 1.9, 2, 2.1 (from top to bottom), $\Omega_0 = 0$, and $\Gamma = 0, \ldots, 0.2$.

T, indicating the $\overline{c} \propto \sqrt{T}$ dependence. While this increase is monotonous till $T \to 0$ for the nonrandom case, in the random system there is only a finite region of T where this increase of $\overline{c}/T$ can be observed. At lower T again the $\overline{c} \propto T$ regime sets in, i.e., the randomness destroys the $\sqrt{T}$ dependence in favor of the T dependence as $T \to 0$. A similar behavior can be found for K values near $K_{\text{crit}} = 2$, e.g., at $K = 1.9$ or 2.1, i.e., we observe the $\sqrt{T}$ dependence for the low-temperature specific heat in a finite temperature range below the high-temperature maximum. That is the typical quantum critical behavior appearing in the vicinity of a quantum critical point.[1–3] Interestingly, in the specific model under consideration for small randomness there is a second maximum for $\overline{c}/T$ (but not for $\overline{c}$) at a lower temperature $T^{\star}$ (which is a reminiscence of the singularity for $K = K_{\text{crit}}$ at $T = 0$) before the $\overline{c} \propto T$ regime sets in at very low temperatures. According to the above discussion for Figs. 5(b), 5(c), and 5(d), we conclude that for the system at $K = K_{\text{crit}}$ at low but finite temperatures the randomness has a similar effect as shifting the nonrandom system slightly away from the quantum critical point. Note that further increasing of Γ removes the low-temperature maximum in $\overline{c}/T$ and also the critical-like $\sqrt{T}$ behavior of $\overline{c}$ disappears, see the curves for $\Gamma = 0.1$ in panels for $K = 1.9$, 2.1 of Fig. 5.

The temperature dependence of the static transverse susceptibility $\overline{\chi_{zz}}$ shown in Fig. 6 exhibits many similarities to that of $\overline{c}/T$ discussed above. In the nonrandom case it is known[16] that for $K = K_{\text{crit}}$ one has $\chi_{zz} \propto 1/\sqrt{T}$ (critical behavior) as $T \to 0$, whereas χ_{zz} remains finite at $T = 0$ for noncritical values of K. For K around K_{crit} a reminiscent of the critical behavior emerges in the low-temperature region starting from certain finite temperatures. For small nonzero Γ, $\overline{\chi_{zz}}$ may exhibit the critical behavior in a certain temperature range starting from finite temperatures if K is equal to or is close to K_{crit}, see the curves for $\Gamma = 0.01$ in panels $K = 1.9$, 2, 2.1 of Fig. 6.

We can use the above-discussed observations of the temperature profiles of $\overline{c}/T$ and $\overline{\chi_{zz}}$ to construct a phase diagram of the random quantum spin chain (2.1), (2.2), i.e., to determine the quantum critical region in the K–T half-plane; see Fig. 7. As an indicator of the critical (i.e., $\sqrt{T}$-like) behavior we choose the value of the derivative $-\partial(\overline{c}/T)/\partial T$. To be more specific, we use the circumstance that, for K in the vicinity of K_{crit}, and small $\Gamma \geqslant 0$, $\overline{c}/T$ exhibits a maximum at $T^{\star}$ (for $K = K_{\text{crit}}$, $\Gamma = 0$ it is a divergency at $T = 0$) and a $1/\sqrt{T}$-like decrease (due to $\overline{c} \propto \sqrt{T}$) in a certain temperature region above $T^{\star}$. As discussed above this behavior is a trace of the quantum critical point. The plots shown in Fig. 7 are based on a quantitative analysis of $-\partial(\overline{c}/T)/\partial T$ and show the value of $-\partial(\overline{c}/T)/\partial T$ as gray-scale plots. All white areas in this figure belong to negative values of $-\partial(\overline{c}/T)/\partial T$. The lower boundary of the quantum critical region is related to $T^{\star}$ (the temperature where the low-temperature maximum of $\overline{c}/T$ is located), since for $T < T^{\star}$ one has $-\partial(\overline{c}/T)/\partial T < 0$, whereas already for T slightly above $T^{\star}$ the derivative $-\partial(\overline{c}/T)/\partial T > 0$ becomes quite large. As a result, the lower boundary of the quantum critical region is quite sharp in Fig. 7. Note that for $\Gamma = 0$ our plot reproduces the typical picture for a quantum critical region.[1–3] For small $\Gamma \geqslant 0$
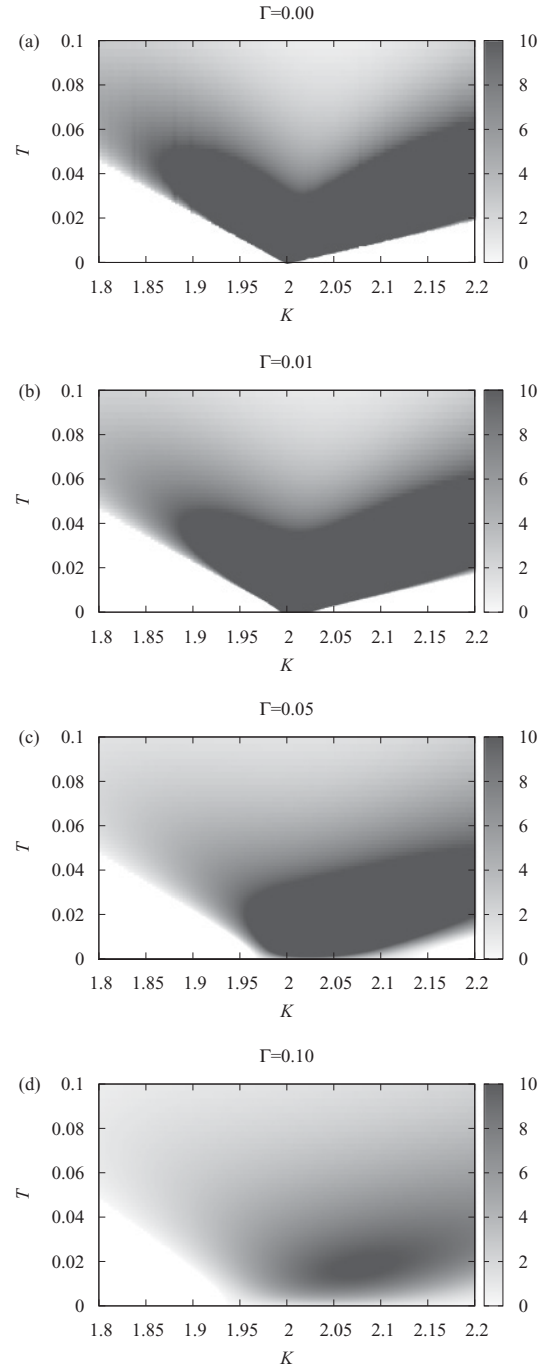

FIG. 7. Critical region as indicated by the value of $-\partial(\overline{c}/T)/\partial T > 0$ in the half-plane K–T for the spin model (2.1), (2.2) with $J = 1$, $\Omega_0 = 0$ and $\Gamma = 0$, 0.01, 0.05, 0.1 (from top to bottom). See further explanations in the main text.

the lower boundaries in the K–T half-plane remain nearly straight lines with different slopes ≈ -0.225 and ≈ 0.096 below and above $K = 2$, respectively. We compare these lower boundaries for various strengths of disorder Γ in Fig. 8, where the numerically determined values of $T^{\star}$ as a function of K are shown. It is obvious that a noticeable change in the slope is observed only in a small vicinity of the $K = 2$. On the other hand, the upper boundary of the quantum critical region is not sharp, since $-\partial(\overline{c}/T)/\partial T$
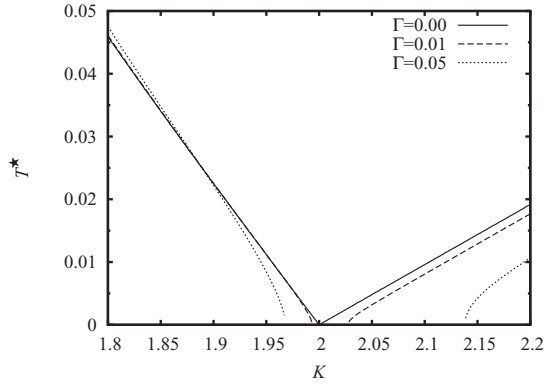
FIG. 8. The lower boundary of the quantum critical region determined by the position of the maximum $T^\star$ of $\overline{c}/T$ for the spin model (2.1), (2.2) with $J = 1$, $\Omega_0 = 0$, and $\Gamma = 0$, 0.01, 0.05.

varies smoothly, if the temperature is further growing. From Fig. 7 it is obvious that for small randomness (see the panel for $\Gamma = 0.01$ in Fig. 7 and the corresponding curves in Fig. 8) at low temperatures the area, where signatures of quantum critical behavior can be observed, is enlarged, whereas a further increase of randomness then leads to a shrinking of that area. For $\Gamma \gtrsim 0.1$ the signatures of quantum criticality completely disappear.

We have to say in the end, that the adopted criterion to indicate the effect of randomness on quantum critical behavior represents only one possibility. In fact, with this criterion we only indicate a region where the specific heat $\overline{c}$ behaves like T^α with $\alpha < 1$ and claim that such a behavior is a remnant of the quantum critical one in the nonrandom model when $\alpha = 1/2$.

V. GENERALIZATION OF THE MODEL

Our consideration until now was restricted to the XX two-site interaction and the $XZX + YZY$ three-site interaction [see Eq. (2.1)] with a Lorentzian probability distribution of the random transverse field, which allows the exact calculation of averaged density of states. In this section we want to generalize the model by (i) extending the Hamiltonian and (ii) considering general probability distributions.

First we illustrate the extension of the Hamiltonian. We can add to the Hamiltonian (2.1) a Dzyaloshinskii–Moriya two-site interaction with the strength D_n and a $XZY - YZX$ three-site interaction with the strength E_n,

$$
\begin{aligned}
H = \sum_n \Big[& J_n \left(s_n^x s_{n+1}^x + s_n^y s_{n+1}^y \right) \\
& + D_n \left(s_n^x s_{n+1}^y - s_n^y s_{n+1}^x \right) \\
& + K_n \left(s_n^x s_{n+1}^z s_{n+2}^x + s_n^y s_{n+1}^z s_{n+2}^y \right) \\
& + E_n \left(s_n^x s_{n+1}^z s_{n+2}^y - s_n^y s_{n+1}^z s_{n+2}^x \right) \Big] + \sum_n \Omega_n s_n^z. \quad (5.1)
\end{aligned}
$$

In fermionic representation Eq. (5.1) reads

$$
\begin{aligned}
H = \sum_n \Big[& \mathcal{A}_n \left(c_n^\dagger c_n - \frac{1}{2} \right) + (\mathcal{B}_n c_n^\dagger c_{n+1} + \text{H.c.}) \\
& + (\mathcal{C}_n c_n^\dagger c_{n+2} + \text{H.c.}) \Big],
\end{aligned} \quad (5.2)
$$

where $\mathcal{A}_n = \Omega_n$, $\mathcal{B}_n = (J_n + iD_n)/2$, and $\mathcal{C}_n = -(K_n + iE_n)/4$. Comparing Eq. (5.2) with Eq. (2.3) we conclude that for a Lorentzian probability of Ω_n and uniform parameters $J_n = J$, $D_n = D$, $K_n = K$, and $E_n = E$ the formula (3.6) for the averaged Green function is valid also for the generalized model (5.1) if we change $J \cos \kappa - (K/2) \cos(2\kappa) \to J \cos \kappa + D \sin \kappa - (K/2) \cos(2\kappa) - (E/2) \sin(2\kappa)$. Further analysis can be performed as in the previous sections. Although the results obtained from the exact averaged density of states are more general now, they do not give basically new features in comparison to those discussed above.

So far our discussion has been referred to a special kind of randomness, i.e., to a Lorentzian transverse field. Only in this case we can provide an exact analysis of the thermodynamics of the spin model. However, it is possible to analyze some global properties of the averaged density of states (which imply corresponding properties of the spin chain) for an arbitrary inhomogeneous spin-1/2 XX chain with three-site interactions in a transverse field (5.1). For that we consider the moments of the density of states (3.1),[33]

$$
\begin{aligned}
M^{(0)} &= \int d\omega \rho(\omega) = \frac{1}{N} \sum_{n=1}^N \langle \{c_n, c_n^\dagger\} \rangle = 1, \\
M^{(1)} &= \int d\omega \omega \rho(\omega) = \frac{1}{N} \sum_{n=1}^N \langle \{[c_n, H], c_n^\dagger\} \rangle, \\
M^{(2)} &= \int d\omega \omega^2 \rho(\omega) = \frac{1}{N} \sum_{n=1}^N \langle \{[[c_n, H], H], c_n^\dagger\} \rangle, \\
M^{(3)} &= \int d\omega \omega^3 \rho(\omega) = \frac{1}{N} \sum_{n=1}^N \langle \{[[[c_n, H], H], H], c_n^\dagger\} \rangle,
\end{aligned}
$$

$$(5.3)$$

etc. Calculating the right-hand sides in Eq. (5.3) with the Hamiltonian (5.2) we find

$$
M^{(1)} = \frac{1}{N} \sum_n \mathcal{A}_n,
$$

$$
M^{(2)} = \frac{1}{N} \sum_n \left(\mathcal{A}_n^2 + |\mathcal{C}_{n-2}|^2 + |\mathcal{B}_{n-1}|^2 + |\mathcal{B}_n|^2 + |\mathcal{C}_n|^2 \right),
$$

$$
\begin{aligned}
M^{(3)} = \frac{1}{N} \sum_n \Big[& |\mathcal{C}_{n-2}|^2 \mathcal{A}_{n-2} + |\mathcal{B}_{n-1}|^2 \mathcal{A}_{n-1} \\
& + \mathcal{A}_n^3 + 2(|\mathcal{C}_{n-2}|^2 + |\mathcal{B}_{n-1}|^2 + |\mathcal{B}_n|^2 + |\mathcal{C}_n|^2) \mathcal{A}_n \\
& + |\mathcal{B}_n|^2 \mathcal{A}_{n+1} + |\mathcal{C}_n|^2 \mathcal{A}_{n+2} \\
& + 2\Re(\mathcal{C}_{n-2}^* \mathcal{B}_{n-2} \mathcal{B}_{n-1} + \mathcal{C}_{n-1}^* \mathcal{B}_{n-1} \mathcal{B}_n + \mathcal{C}_n^* \mathcal{B}_n \mathcal{B}_{n+1}) \Big].
\end{aligned}
$$

$$(5.4)$$

The moments of the random-averaged density of states $\overline{\rho(\omega)}$ follow from Eq. (5.4) after a corresponding averaging.

We may use the derived moments of the density of states (5.4) to examine some general properties of the (homogeneous or inhomogeneous) spin chain (5.1). For example, the ground-state transverse magnetization is given by the formula

$$
m_z = -\int d\omega \rho(\omega) \left[\theta(\omega) - \frac{1}{2} \right]; \quad (5.5)
$$

see Eq. (4.4). It has been shown that the uniform spin model (5.1) may exhibit a nonzero transverse magnetization m_z in zero transverse field $\Omega_n = \Omega_0 = 0$.[15–17,34] From Eq. (5.5) it is clear that $m_z \neq 0$ at zero field if the density of states is asymmetric, i.e., if the third moment of the density of states at zero field is nonzero.

In the uniform (nonrandom) case we have $M^{(3)} = \mathcal{A}^3 + 6(|\mathcal{B}|^2 + |\mathcal{C}|^2)\mathcal{A} + 6\Re(\mathcal{C}^*\mathcal{B}^2)$, or in the zero-field case $M^{(3)} = 6\Re(\mathcal{C}^*\mathcal{B}^2) = -(3/8)[(J^2 - D^2)K + 2JDE]$. From the latter formula it is obvious that only three-site interactions may lead to nonzero magnetization. More precisely, the $XZX + YZY$ interaction if $J^2 \neq D^2$ or the $XZY - YZX$ interaction if $JD \neq 0$ leads to $m_z \neq 0$ at zero field. Formulas for the moments of the density of states (5.4) permit us to examine the effect of randomness on this property. An example of such analysis is given in Ref. 15 where some consequences of the correlated off-diagonal and diagonal disorder were discussed.

Finally we note that the high-temperature properties of the spin model are determined by the lower moments of the density of states [see Eq. (3.1)], and therefore the thermodynamic quantities in the high-temperature limit can be examined accurately for any type of disorder on the basis of Eq. (5.4).

VI. CONCLUSIONS

We have considered a random spin-1/2 XX chain with three-site interactions. For a random on-site transverse field with Lorentzian probability distribution we have calculated exactly the random-averaged density of states and the corresponding random-averaged thermodynamic quantities of the model. For arbitrary inhomogeneous Hamiltonian parameters we have calculated the three first moments of the density of states that determine some general properties of the spin model and yield its thermodynamic quantities in the high-temperature limit. The effect of a random transverse field on the ground-state magnetization process and on the temperature behavior of the specific heat and static transverse susceptibility has been analyzed. As a main result we have discussed how the quantum critical behavior of the spin-1/2 XX chain with three-site interactions is modified by randomness. While for large enough randomness all signatures of quantum critical behavior disappear, we find even a slightly enlarged temperature area for very small randomness, where such signatures can be observed.

Finally, we have to underline that our analytical findings are restricted to the random-averaged density of states and thermodynamic quantities. To our best knowledge, almost all applications of Lloyd's model are restricted to one-particle quantities that can be obtained rigorously. The calculation of the two-particle quantities meets notorious difficulties and requires approximations; see e.g., Ref. 35. On the other hand, other quantities of interest that are not related to the one-particle Green functions (3.3) but are important for following final outcomes of introduced randomness (e.g., two-spin correlation functions) may be examined only numerically for finite chains;[36] see also Ref. 37. However, numerical studies are beyond the scope of the present paper and will be reported separately.

APPENDIX: THE ROOTS OF Eq. (3.8)

In this Appendix we give explicit expressions for the roots of Eq. (3.8). They read:

$$\{z_1, z_2, z_3, z_4\} = \left\{ \frac{\frac{J}{K} - g - \sqrt{\left(\frac{J}{K} - g\right)^2 - 4}}{2}, \right.$$
$$\frac{\frac{J}{K} + g - \sqrt{\left(\frac{J}{K} + g\right)^2 - 4}}{2},$$
$$\frac{\frac{J}{K} - g + \sqrt{\left(\frac{J}{K} - g\right)^2 - 4}}{2},$$
$$\left. \frac{\frac{J}{K} + g + \sqrt{\left(\frac{J}{K} + g\right)^2 - 4}}{2} \right\}, \quad \text{(A1)}$$

with $g = \sqrt{(J/K)^2 - (4/K)(\omega - \Omega_0 + i\Gamma) + 2}$ in the case of the retarded Green functions (3.3) or $g = \sqrt{(J/K)^2 - (4/K)(\omega - \Omega_0 - i\Gamma) + 2}$ in the case of the advanced Green functions (3.3).

[1]S. L. Sondhi, S. M. Girvin, J. P. Carini, and D. Shahar, Rev. Mod. Phys. **69**, 315 (1997).

[2]S. Sachdev, *Quantum Phase Transitions* (Cambridge University Press, Cambridge, 1999).

[3]S. Sachdev, in *Quantum Magnetism*, edited by U. Schollwöck, J. Richter, D. J. J. Farnell, and R. F. Bishop, Lecture Notes in Physics **645** (Springer, Berlin, 2004), p. 381.

[4]P. Pfeuty, Ann. Phys. (NY) **57**, 79 (1970).

[5]J. M. Luck, J. Stat. Phys. **72**, 417 (1993).

[6]B. K. Chakrabarti, A. Duta, and P. Sen, *Quantum Ising Phases and Transitions in Transverse Ising Models* (Springer-Verlag, Berlin, 1996).

[7]F. Iglói, L. Turban, D. Karevski, and F. Szalma, Phys. Rev. B **56**, 11031 (1997).

[8]O. Derzhko, J. Richter, T. Krokhmalskii, and O. Zaburannyi, Phys. Rev. B **66**, 144401 (2002); Phys. Rev. E **69**, 066112 (2004).

[9]E. Lieb, T. Schultz, and D. Mattis, Ann. Phys. (NY) **16**, 407 (1961); S. Katsura, Phys. Rev. **127**, 1508 (1962); **129**, 2835 (1963).

[10] S. Watarai and T. Matsubara, J. Phys. Soc. Jpn. **53**, 3648 (1984).

[11] R. R. Levitskii, R. O. Sokolovskii, and S. I. Sorokov, Condens. Matter Phys. (L'viv) No. **10**, 67 (1997).

[12] R. M. Morra, R. L. Armstrong, and D. R. Taylor, Phys. Rev. Lett. **51**, 809 (1983).

[13] M. Kenzelmann, R. Coldea, A. A. Tennant, D. Visser, M. Hofmann, P. Smeibidl, and Z. Tylczynski, Phys. Rev. B **65**, 144432 (2002).

[14] A. Kitaev, Ann. Phys. (NY) **321**, 2 (2006); W. Brzezicki and A. M. Oleś, Phys. Rev. B **80**, 014405 (2009); A. Saket, S. R. Hassan, and R. Shankar, *ibid*. **82**, 174409 (2010).

[15] D. Gottlieb and J. Rössler, Phys. Rev. B **60**, 9232 (1999); O. Derzhko, J. Richter, and V. Derzhko, Ann. Phys. (Leipzig) **8**, SI-49 (1999), e-print arXiv:cond-mat/9908425.

[16] I. Titvinidze and G. I. Japaridze, Eur. Phys. J. B **32**, 383 (2003).

[17] P. Lou, W.-C. Wu, and M.-C. Chang, Phys. Rev. B **70**, 064405 (2004); P. Lou, Phys. Status Solidi B **241**, 1343 (2004).

[18] M. Suzuki, Phys. Lett. A **34**, 338 (1971); Prog. Theor. Phys. **46**, 1337 (1971).

[19] P. Lloyd, J. Phys. C **2**, 1717 (1969).

[20] H. Nishimori, Phys. Lett. A **100**, 239 (1984); K. Okamoto, J. Phys. Soc. Jpn. **59**, 4286 (1990); O. Derzhko and T. Verkholyak, Phys. Status Solidi B **200**, 255 (1997); Fiz. Nizk. Temp. (Kharkiv) **23**, 977 (1997); Low Temp. Phys. **23**, 733 (1997).

[21] W. John and J. Schreiber, Phys. Status Solidi B **66**, 193 (1974); J. Richter, K. Handrich, and J. Schreiber, *ibid*. **68**, K61 (1975); J. Richter, J. Schreiber, and K. Handrich, *ibid*. **74**, K125 (1976); J. Richter, *ibid*. **87**, K89 (1978); **99**, K13 (1980).

[22] O. Derzhko and J. Richter, Phys. Lett. A **222**, 338 (1996); Phys. Rev. B **55**, 14298 (1997); **59**, 100 (1999).

[23] D. S. Fisher, Phys. Rev. Lett. **69**, 534 (1992); Phys. Rev. B **51**, 6411 (1995).

[24] J. K. Pachos and M. B. Plenio, Phys. Rev. Lett. **93**, 056402 (2004); J. K. Pachos and E. Rico, Phys. Rev. A **70**, 053620 (2004).

[25] T. Krokhmalskii, O. Derzhko, J. Stolze, and T. Verkholyak, Phys. Rev. B **77**, 174404 (2008).

[26] W. W. Cheng and J.-M. Liu, Phys. Rev. A **82**, 012308 (2010); F. G. Ribeiro, J. P. de Lima, and L. L. Gonçalves, J. Magn. Magn. Mater. **323**, 39 (2011).

[27] D. N. Zubarev, *Njeravnovjesnaja Statistitchjeskaja Tjermodinamika* (Nauka, Moscow, 1971) [in Russian].

[28] G. Rickayzen, *Green's Functions and Condensed Matter* (Academic, London, 1991).

[29] G. D. Mahan, *Many-Particle Physics* (Plenum, New York, 1993).

[30] D. J. Thouless, J. Phys. C **5**, 77 (1972).

[31] In general, not all one-particle states in one dimension in the presence of disorder should become localized, see e.g., G. Theodorou and M. H. Cohen, Phys. Rev. B **13**, 4597 (1976); T. P. Eggarter and R. Riedinger, *ibid*. **18**, 569 (1978); C. M. Soukoulis and E. N. Economou, *ibid*. **24**, 5698 (1981) (off-diagonal disorder); H. Hermann and J. Schreiber, Phys. Status Solidi B **67**, K93 (1975) (correlated off-diagonal Lorentzian disorder). In some cases the localization length may diverge at certain energes resulting in singularities of the density of states and a more subtle effect of randomness on quantum phases and phase transitions between them. For further examples of one-dimensional disordered systems see also M. Yamanaka, Y. Avishai, and M. Kohmoto, Phys. Rev B **54**, 228 (1996); R. H. McKenzie, Phys. Rev. Lett. **77**, 4804 (1996); J. E. Bunder and R. H. McKenzie, Phys. Rev. B **60**, 344 (1999).

[32] J. Schulenburg, A. Honecker, J. Schnack, J. Richter, and H.-J. Schmidt, Phys. Rev. Lett. **88**, 167207 (2002); J. Richter, J. Schulenburg, A. Honecker, J. Schnack, and H.-J. Schmidt, J. Phys.: Condens. Matter **16**, S779 (2004); R. Schmidt, J. Richter, and J. Schnack, J. Magn. Magn. Mater. **295**, 164 (2005).

[33] K. Elk and W. Gasser, *Die Methode der Greenschen Funktionen in der Festkörperphysik* (Akademie-Verlag, Berlin, 1979), p. 47 [in German]; W. Gasser, E. Heiner, and K. Elk, *Greensche Funktionen in Festkörper- und Vielteilchenphysik* (Wiley-VCH, Berlin, 2001), p. 59 [in German].

[34] For (nonrandom) spin-1/2 XX chains with the $XZY - YZX$ three-site interactions it is immediately clear that $m_z = 0$ if $\Omega = 0$. Really, consider a spin rotation around the y axis by π, $s^y \to s^y$, $s^x \to -s^x$, $s^z \to -s^z$. As a result, the Hamiltonian $H(J,E,\Omega)$ transforms into the Hamiltonian $H(J,E,-\Omega)$, and for $\Omega = 0$ we have $\langle s^z \rangle_{J,E,\Omega=0} = -\langle s^z \rangle_{J,E,-\Omega=0} = 0$.

[35] M. Saitoh, Prog. Theor. Phys. **45**, 746 (1971).

[36] O. Derzhko and T. Krokhmalskii, Phys. Rev. B **56**, 11659 (1997); Phys. Status Solidi B **208**, 221 (1998); A. P. Young, Phys. Rev. B **56**, 11691 (1997); P. Henelius and S. M. Girvin, *ibid*. **57**, 11457 (1998); X. Jia and S. Chakravarty, *ibid*. **74**, 172414 (2006).

[37] A. Furusaki, M. Sigrist, P. A. Lee, K. Tanaka, and N. Nagaosa, Phys. Rev. Lett. **73**, 2622 (1994); K. Hamacher, J. Stolze, and W. Wenzel, *ibid*. **89**, 127202 (2002); T. Verkholyak, O. Derzhko, T. Krokhmalskii, and J. Stolze, Phys. Rev. B **76**, 144418 (2007).